

PROCEEDINGS OF SPIE

[SPIDigitalLibrary.org/conference-proceedings-of-spie](https://spiedigitallibrary.org/conference-proceedings-of-spie)

The Tenerife Microwave Spectrometer (TMS) experiment: studying the absolute spectrum of the sky emission in the 10-20GHz range

Rubiño Martín, José Alberto, Alonso Arias, Paz, Hoyland, Roger, Aguiar-González, Marta, De Miguel-Hernández, Javier, et al.

José Alberto Rubiño Martín, Paz Alonso Arias, Roger J. Hoyland, Marta Aguiar-González, Javier De Miguel-Hernández, Ricardo T. Génova-Santos, Maria F. Gomez-Reñasco, Federica Guidi, Patricia Fernández-Izquierdo, Mateo Fernández-Torreiro, Pablo A. Fuerte-Rodriguez, Carlos Hernandez-Montegudo, Carlos H. López-Caraballo, Angeles Perez-de-Taoro, Michael W. Peel, Rafael Rebolo, Antonio Zamora-Jimenez, Eduardo D. González-Carretero, Carlos Colodro-Conde, Cristina Pérez-Lemus, Rafael Toledo-Moreo, David Pérez-Lizán, Francesco Cuttaia, Luca Terenzi, Cristian Franceschet, Sabrina Realini, Jens Chluba, Gaizka Murga-Llano, Ruben Sanquirce-Garcia, "The Tenerife Microwave Spectrometer (TMS) experiment: studying the absolute spectrum of the sky emission in the 10-20GHz range," Proc. SPIE 11453, Millimeter, Submillimeter, and Far-Infrared Detectors and Instrumentation for Astronomy X, 114530T (13 December 2020); doi: 10.1117/12.2561309

SPIE.

Event: SPIE Astronomical Telescopes + Instrumentation, 2020, Online Only

The Tenerife Microwave Spectrometer (TMS) experiment: studying the absolute spectrum of the sky emission in the 10–20 GHz range

José Alberto Rubiño-Martín^{a,b}, Paz Alonso-Arias^{a,b}, Roger J. Hoyland^{a,b}, Marta Aguiar-González^{a,b}, Javier de-Miguel-Hernández^{a,b}, Ricardo T. Génova-Santos^{a,b}, Maria F. Gómez-Reñasco^{a,b}, Federica Guidi^{a,b}, Patricia Fernández-Izquierdo^a, Mateo Fernández-Torreiro^{a,b}, Pablo A. Fuerte-Rodríguez^a, Carlos Hernández-Monteagudo^{a,b}, Carlos H. López-Caraballo^{a,b,j}, Angeles Perez-de-Taoro^a, Michael W. Peel^{a,b}, Rafael Rebolo^{a,b,i}, Antonio Zamora-Jimenez^a, Eduardo D. González-Carretero^a, Carlos Colodro-Conde^{a,c}, Cristina Pérez-Lemus^d, Rafael Toledo-Moreo^d, David Pérez-Lizán^d, Francesco Cuttaia^e, Luca Terenzi^e, Cristian Franceschet^f, Sabrina Realini^f, Jens Chluba^g, Gaizka Murga-Llano^h, and Rubén Sanquirc-García^h

^aInstituto de Astrofísica de Canarias, Calle Vía Láctea SN, ES38205 La Laguna, Spain

^bDepartamento de Astrofísica, Universidad de La Laguna, ES38205, La Laguna, Spain

^cIAC Technology, Parque Científico y Tecnológico de Tenerife S.A., Calle Rectora María Luisa Tejedor Salguero. Parque Urbano Las Mantecas, Edificio Nanotec, 38320 La Laguna, Spain

^dEscuela Técnica Superior de Ingeniería de Telecomunicación, Universidad Politécnica de Cartagena, Edif. Antigones, Cartagena, 30202, Spain

^eIstituto Nazionale di Astrofisica, via Gobetti 93/3, 40129 Bologna - Italy

^fUniversità degli Studi di Milano, Via Celoria 16, 20133 Milano, Italy

^gJodrell Bank Centre for Astrophysics, University of Manchester, Oxford Road, Manchester M13 9PL, UK

^hIDOM, Av. Zarandoa 23, 48015 Bilbao, Spain

ⁱConsejo Superior de Investigaciones Científicas (CSIC), Spain

^jINFN–Sezione di Milano, Via Celoria 16, Milano, Italy

ABSTRACT

The Tenerife Microwave Spectrometer (TMS) is a new 10–20 GHz experiment that will be installed at the Teide Observatory (Tenerife, Spain), next to the QUIJOTE CMB experiment.¹ The main TMS scientific driver is to accurately measure absolute distortions of the sky spectrum in the 10–20 GHz frequency range, with special emphasis on the characterization of the absolute synchrotron monopole from our Galaxy, and the possible deviations of the CMB spectrum from a pure blackbody law. TMS will provide an absolute calibration for the QUIJOTE experiment, and it will also serve as a prototype for future instruments of its type, both ground-based and satellites. Among its new instrumental design is an octave bandwidth high quality cryogenic front-end, a thermally stabilized cold black body and a new design of wide-band Fourier transform spectrometer. The spectrometer will have a resolution of 250 MHz, giving 40 spectrally stable sub-bands.

Keywords: cosmic microwave background, polarization, spectrometer, telescopes, instrumentation, cryogenics, temperature control

Corresponding author: J.A. Rubiño-Martín. Email: jalberto@iac.es, Telephone: +34 922 605 276

1. INTRODUCTION

The Cosmic Microwave Background (CMB) provides one of the most powerful tools in modern cosmology to test our understanding of the Universe. Thanks to the observational study of the CMB anisotropies with different experiments over the past decades, we have firmly established the Λ CDM concordance model, entering the so-called “precision cosmology” era.^{2,3} Nowadays, CMB polarization observations offer a new window to the inflationary phase of the Universe, some 10^{-35} s after the Big Bang. Experiments like BICEP/Keck, ACT, SPT, CLASS, PolarBear, GroundBird, Simons Observatory and QUIJOTE are looking for the signature of primordial gravitational waves in the CMB polarization maps. And a number of experiments are planned for the coming years, including ground-based facilities such as QUBIC, LSPE-STRIP, CMB-S4, or space missions, such as Litebird.

However, beyond the CMB polarization, there is also a wealth of almost unexplored information, encoded in small deviations of the CMB energy spectrum from the pure black-body shape, providing new ways to probe the thermal history of our Universe, the inflationary era and the nature of the dark matter.⁴

The CMB radiation observed today is the most perfect black-body radiation ever observed in nature, with a temperature of about 2.726 K. It is a “snapshot” of the radiation at the time of decoupling between matter and radiation in the early Universe. The remarkable measurement of the CMB spectrum by COBE/FIRAS⁷ is rightfully highlighted as a crucial confirmation of the Big Bang cosmology. However, the standard cosmological model predicts unavoidable distortions in the CMB spectrum arising throughout most of the history of the Universe, from now to the blackbody photosphere of the Universe at $z \sim 2 \times 10^6$ (see e.g. 8,9 and references therein). In fact, most of the information contained in the CMB spectrum is inaccessible by any other astrophysical means. Therefore, the measurement of the absolute CMB spectrum will open an unexplored window

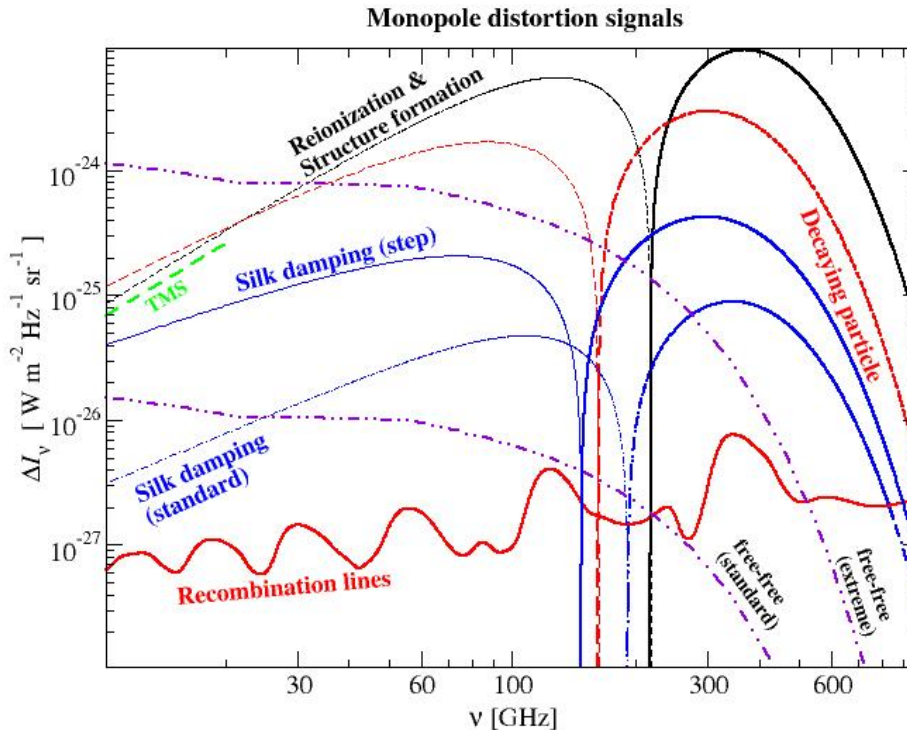


Figure 1. Spectral distortions for different scenarios. Thick lines denote positive, and thinner lines negative signals. The largest distortion corresponds to the case of the heating of medium during reionization and structure formation, using $y = 5 \times 10^{-7}$. The expected value is likely higher than this.⁵ The decaying dark-matter particle scenario corresponds to a lifetime of 3.6×10^9 s for the dark matter particle. The figure has been adapted from [6]. The contribution of Galactic and extra-galactic foregrounds is not included. In the green colour, we show the predicted sensitivity of the proposed TMS spectrometer in the 10–20 GHz range, after 100 h of integration.

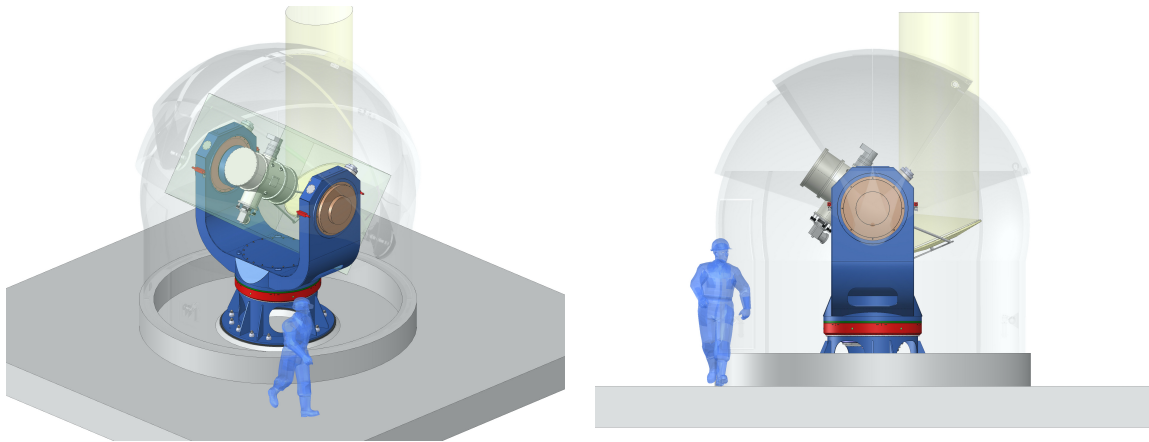


Figure 2. A 3D drawing of the TMS experiment, with its dome, platform and instrument.

to the early Universe.¹⁰ Among other scenarios, spectral distortions (see Figure 1) will allow us to explore the reionization epoch; to constrain the inflaton at scales well below 1 Mpc; to study decaying and annihilating relics, metals during the dark ages or the cosmological recombination radiation. For a more detailed review, see [4] and reference therein.

Since the remarkable measurement of the CMB spectrum by COBE/FIRAS, the CMB community has been focused in the characterization of the spatial fluctuations of the signal. Absolute measurements of the CMB at longer wavelengths than COBE/FIRAS have been carried out with few ground-based and balloon-borne experiments (see e.g. 11–14). The constraints from the ARCADE 2 experiment [15] set upper limits to CMB spectral distortions of $\mu < 6 \times 10^{-4}$ and $|Y_{\text{ff}}| < 10^{-4}$, although the most remarkable result is an unexplained residual signal,^{16–19} which might be due to an underestimated foreground contribution in the form of a power law with amplitude 18.4 ± 2.1 K at 0.31 GHz and a spectral index of -2.57 ± 0.05 .

New spacecraft proposals like PIXIE,²⁰ PRISM⁶ and others⁴ show promise in the detection of the majority of these distortions in the future (beyond 2030), but at this moment, there is a window of opportunity for new experiments to explore new observational windows and technological solutions. The measurement of the CMB spectrum to the accuracy that will reveal interesting science (microK variations) is particularly difficult because there are many systematic effects that lead to observed signals higher than this level. Moreover, ground-based experiments can provide low frequency observations ($\nu \lesssim 20$ GHz), which are hard to access from space. The proposed TMS is a first step towards improving the required solutions, but at the same time, providing sufficient sensitivity in a scientifically important frequency band to address some specific open questions.

2. PROJECT BASELINE

The TMS is an ultra-high sensitive radio-spectrometer that will observe in the 10–20 GHz band with an angular resolution of $\sim 3^\circ$ from the Teide Observatory (OT) at an altitude of 2400 m, in Tenerife (Spain). This site has a long tradition (more than 35 years) in the study of CMB anisotropies, with experiments like the Tenerife radiometers (1984–2000), the IAC-Bartol (1994–1997), the JBO-IAC two-element 30 GHz interferometer (1997–2002), the COSMOSOMAS experiment (1998–2007), the Very Small Array interferometer (2000–2008), the QUIJOTE experiment (2012–), Groundbird (2019–) and LSPE-STRIP (2021–). The median precipitable water vapour (PWV) is 3.5 mm, reaching values below 1.7 mm during 25 per cent of the time.²¹

TMS is led by the Instituto de Astrofísica de Canarias, with an instrumental participation from the INAF group (Bologna), the University of Milano, the Universidad Politécnica de Cartagena (UPCT) and the IDOM company. The project is fully funded. The TMS instrument consists of a cryogenically cooled front-end covering the whole band of 10–20 GHz through each of two pseudo-correlators that are stabilized with a 4 K reference load. The radiometers are heterodyne and the band is initially divided up into 4 sub-bands in order to be directly



Figure 3. Left: Location of the former VSA platform at the Teide Observatory. The TMS dome will be installed in the central enclosure (marked as TMS). Right: Fiberglass AllSky dome installed for the GroundBird experiment at the Teide Observatory. The TMS dome, to be installed in the second enclosure, is similar to this one.

acquired through ultrafast ADCs and FPGA. The spectrometer is to be mounted in the multi-purpose platform described in the next section (see Figure 2).

Table 1 summarizes the basic (nominal) characteristic of the TMS. The expected system temperature is 20 K, accounting for instrument contributions and sky emission (CMB and atmosphere). The expected FWHM of the beam with optics is approximately 3° in the center of the band, and the spectral resolution is 250 MHz. With these numbers, the expected sensitivity in each of the 40 sub-channels is $\sim 2 \text{ mK s}^{1/2}$, allowing us to reach the level of $10^{-25} \text{ W m}^{-2} \text{ Hz}^{-1} \text{ sr}^{-1}$ ($= 10 \text{ Jy/sr}$) at 10 GHz after 100 h on target. After two years of operations, this sensitivity could be achieved in about 3000 deg^2 . Even though the absolute calibration of the instrument will be ultimately limited by our ability to remove the atmospheric contamination and to control its stability, the TMS has been optimised to provide a very precise relative calibration between all its frequency sub-bands.

Table 1. Nominal characteristics of the TMS experiment. See text for details.

Frequency range [GHz]	10.0–20.0
Frequency resolution [GHz]	0.25
Spectral resolution, $R = \lambda/\Delta\lambda$	60.0
T_{sys} [K]	22.0
Beam FWHM [deg]	3.0
Cross-polarization (whole band)	$< -30 \text{ dB}$
Sidelobe levels (whole band)	$< -25 \text{ dB}$
NEP per frequency channel [$\text{mK s}^{1/2}$]	1.97
Average sensitivity in 100 h integration at 10 GHz [Jy/sr]	10.3

Although it has not been optimized for this purpose, the TMS will also have polarimetric capabilities, thanks to the use of the two orthogonal polarizations of the OMTs. By combining the TMS outputs in the post-processing stage, we should be able to reconstruct the linear polarization spectra (Stokes Q and U parameters) with only a small penalty of root 2 more noise. Although the majority of the spectral distortions discussed in Section 1 (and Figure 1) are unpolarized, this polarization capability is of importance for modelling foregrounds.

3. EXPERIMENT DESCRIPTION

3.1 Enclosure

The TMS experiment will be installed in the former platform of the VSA experiment.²² The ground screen as well as the control room, already existing, will be reused (see Figure 3, left panel). The location will be close to the

existing QUIJOTE experiment.¹ The TMS instrument and its mount will be integrated inside a fiberglass all-sky dome of 4.5 m (Figure 3, right panel), fitted inside the existing ground shielding, which allows an observation area of the sky of 180°. The foundation of the dome will be isolated from the telescope foundation, to prevent dynamic loads from being transferred one to the other. A feedthrough located in the wall of the dome will allow placement of the compressor and the chiller outside the dome, reducing the thermal load and temperature variation inside the dome. The dome includes several actuators and sensors to control its movement by means of a micro-controller, which will be connected to a server-logger to enable remote operation. In addition, a weather station outside the dome will monitor the environmental conditions at the observatory, allowing an automatic evaluation and closing the dome if necessary.

3.2 Telescope mount and optics

The TMS will be mounted on a multi-purpose alt-azimuth platform that will keep the cryostat at a given elevation angle while scanning around the azimuth axis. The design of the platform is based on the existing QUIJOTE telescopes,¹ and consists of a pedestal that provides the azimuth movement, and a fork (shown in Figure 2). The instrument will be coupled to this fork, allowing the movement in the elevation axis. Although it will be mainly used for the TMS experiment, its design contemplates the possibility of re-using this platform for testing other future experiments. The full mount is now being fabricated by the IDOM company.

The telescope mount guarantees continuous azimuth rotation and a zenith distance from -10° to $+60^\circ$. Similarly to the QUIJOTE telescopes, it could be operated remotely, with a maximum azimuth velocity of 20 deg/s, and a minimum scan speed of 15 arcsec/s. The maximum allowed pointing error during tracking is 1 arcmin (RMS) in 60 minutes. Once the instrument is installed in this platform, the sky signal will be focused on the TMS cryostat window by means of an off-axis parabolic reflector of approximately 1.3 m attached to the instrument. Hence, the platform provides the movement to implement the scanning strategy. The parabola will be machined out of an aluminium block. The backside will be given a honeycomb form to strengthen the parabolic surface and lighten the overall design. The optical design is still being optimised. The optimisation covers the whole band 10–20 GHz. The aim is to minimise cross-polarization, sidelobe level and ellipticity whilst providing a similar FWHM beam over the whole band. Some of these qualities work against each other and the feedhorn response has to be fully adapted. The size, offset angle and shape of the parabola are all being optimised. The parabola will have an edge taper of -20 dB. We are also looking into other possible optical configurations such as a crossed-dragone dual reflector design.

Provision will be made for mounting eccosorb around the parabolic reflector in order to cut out unwanted reflections adding to the sidelobe level and instrument induced polarization. The dome environment will be designed to minimize thermal fluctuations during observation.

3.3 Instrument

The TMS instrument is an ultra-high sensitive radio-spectrometer covering the band between 10–20 GHz through two pseudo-correlators that are stabilized with a 4 K reference load. This pseudo-correlation architecture, along with a switching strategy of the inputs between the reference signal and the signal of interest from the sky, has proven to be particularly robust against $1/f$ gain variations, as proven by the LFI receivers on-board the Planck mission.²³ However, the TMS design removes the need for signal switching by performing an ultra-high speed digital acquisition using a System-on-Chip Field Programmable Gate Array (SoC FPGA). The radiometers are based on a heterodyne architecture and the band is initially divided up into four subbands in order to be directly acquired through the mentioned ultrafast ADCs and FPGA. The data are averaged and then saved offline in a PC that is also responsible for quick-look software written in LABVIEW to monitor the system. A complete and detailed description of the instrument and its current status is presented in [24]. Here we outline the basic characteristics of the instrument.

Figure 4 presents a schematic diagram of the microwave spectrometer for the TMS instrument. A closed cycle helium cooler cools the front-end of the radiometer to 4–10 K, which includes the opto-mechanics, the HEMT-based ultra Low Noise Amplifiers (LNA) and a broadband reference load. Two hybrid couplers are used to provide correlation between the two inputs for each polarization. This Front-End Module (FEM) stage is depicted in the top panel of Fig. 4 with a blue background. The back-end modules (BEMs) are maintained at room

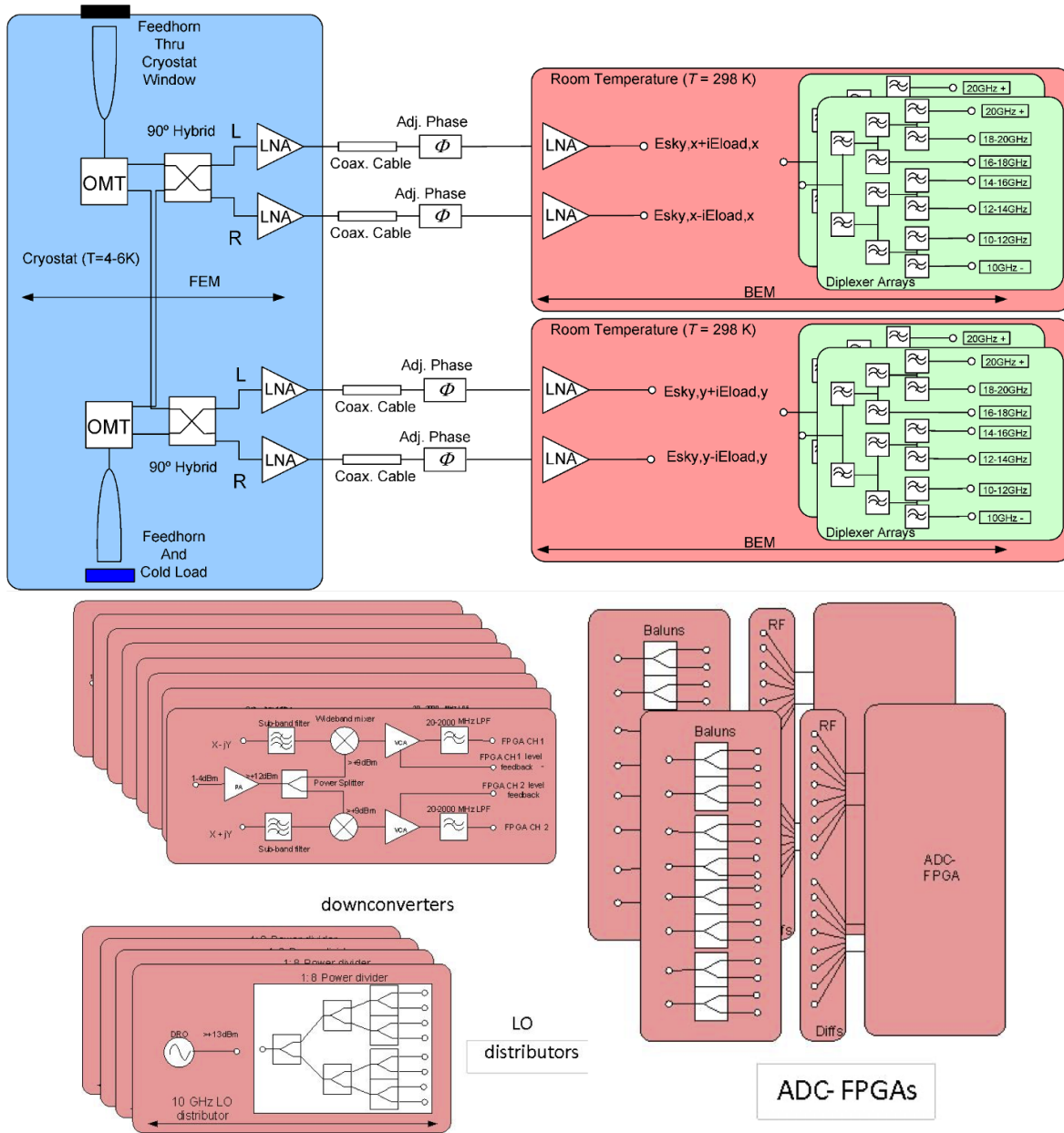


Figure 4. Schematic diagram of the general layout of the TMS instrument. Top: Front-end-module (FEM) and Back-end-module (BEM). Bottom: Down-converters, Local Oscillator distributors and ADC-FPGAs (see text for details).

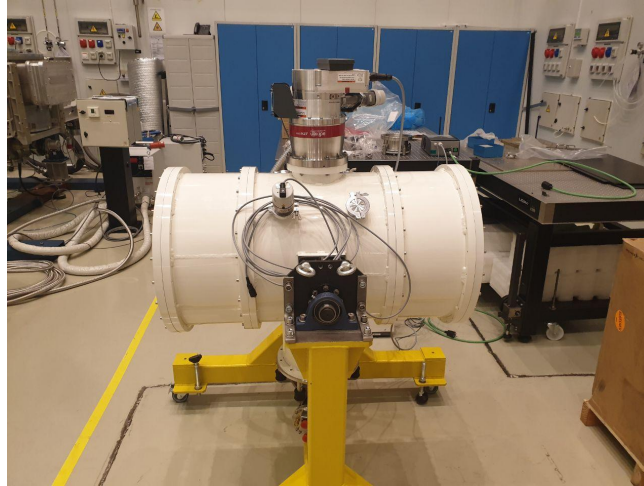


Figure 5. TMS cryostat (vacuum chamber) and cold head, at the IAC workshop.

temperature and contain room temperature microwave amplifiers, frequency division and definition (depicted in the top panel of Fig. 4 in salmon pink). A set of down-conversion modules and LO distribution blocks provide the down conversion of the sub-bands to the FPGA baseband. An FPGA-based module (Xilinx ZCU208) that includes ultrafast analog-to-digital conversion performs all the operations related to direct acquisition, processing, formatting and transmission of the data to a LABVIEW application running in a PC.

3.3.1 Cryostat

The cryostat of the TMS consists of an axis-symmetric vacuum chamber made of AA6061-T6 with internal dimensions of 970 mm in length and 490 mm in diameter. This symmetric design favours the isothermal design constraints on each branch of the comparative radiometric measurement system. It is equipped with an air-cooled Pfeiffer ATH-500M turbomolecular pump and a Sumitomo RDK-415D cold head. All these subsystems are already fabricated since July 2019 (see Figure 5), and tested in a laboratory.²⁴

3.3.2 Opto-mechanical components

The opto-mechanical components of the TMS are in a well-advanced state. The two (identical) feedhorns of the instrument have been already designed and manufactured, using a novel meta-horn design.^{25,26} This design ensures cross polarization and return loss levels below -35 dB and -25 dB across the full 10–20 GHz band, respectively. The horn radiation patterns are being measured in an anechoic chamber at the University of Milano (see details in 24). The design of the OMTs and the 90° hybrid couplers is in process. These components do not exist commercially with the high level of specification required by the TMS. Both OMT and hybrid must have below -25 dB return loss and the insertion loss must be below -0.5 dB across the full octave bandwidth. These components are therefore being designed and fabricated in-house using new technology. In addition to these stringent optical and radiometric constraints, the TMS thermal requirements give rise to requirements on the thermal conductivity of the materials they are made from as well as how they are implemented in the cryostat. The cryostat thermal design is critical to achieve the scientific goals of this project. The difference in temperature between one arm of the optomechanics and the other shall be less than ± 0.5 K. The difference between the Load temperature and the optomechanics shall be also less than ± 0.5 K.

3.3.3 Reference load

The pseudo-correlation scheme of the TMS radiometer uses an internal source to generate a reference signal for continuous comparison with the sky emission received through one of the feedhorns. This subsystem is being developed by the INAF group in Bologna. This cryogenic load shall be a representative blackbody between 10–20 GHz with > 0.999 emissivity, < -30 dB return loss, and shall be held at a temperature between 5–10 K (nominal $T_{\text{load}} = 6$ K) depending on the thermal model derived from the cryostat design. This temperature shall be held to ± 100 mK for the duration of one observing campaign (1 month).

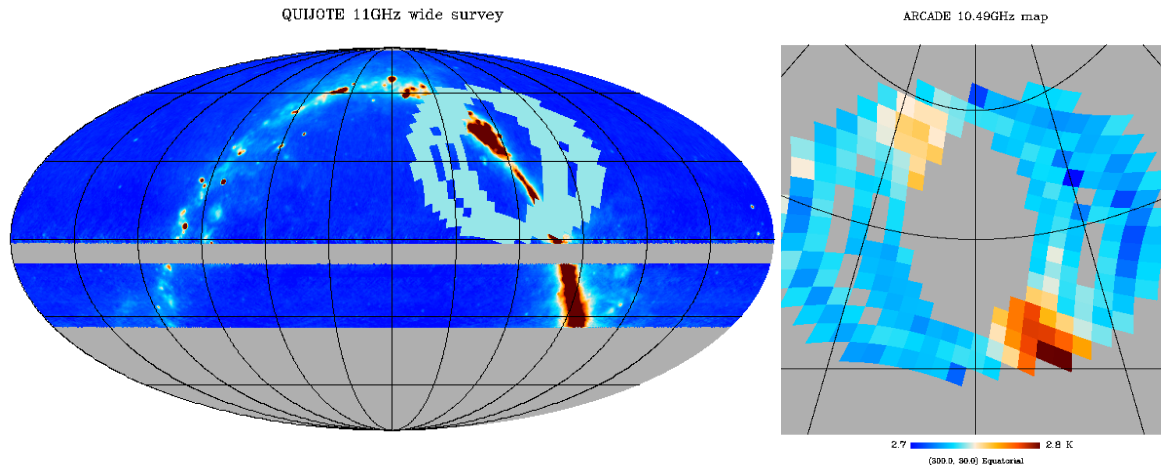


Figure 6. Left: QUIJOTE 11 GHz wide survey map in intensity, in equatorial coordinates [27]. The light-blue area corresponds to the footprint of the ARCADE data [14]. Grey areas correspond to unobserved pixels. Right: ARCADE 10.49 GHz map, in equatorial coordinates (downloaded from LAMBDA).

The final design of the load consists of an array of square-based metal aluminium pyramids coated with CR/MF-117 Eccosorb material (<https://www.laird.com/products>), enhancing the emissivity and temperature homogeneity of the calibrator. Further details are presented in [24] and Alonso-Arias et al. (in prep.). The absolute temperature of the cryogenic load shall be known to ± 15 mK with an appropriate temperature measurement scheme, and using several Lake Shore cryogenic temperature sensors and controllers. The absolute temperature of the load shall be held stable within 1 mK for periods of 1 hr observation.

3.3.4 Data acquisition system

The data acquisition system (DAS) for the TMS will be based on a SoC-FPGA, to provide the required capability to digitize and decompose the spectral band between 10–20 GHz, while filtering and correcting possible radio-interference signals. It will take advantage of the new Xilinx ZCU208 Ultrascale, which presents up to eight 2.5 GHz input channels. A more detailed description of the DAS system can be found in [24]. The development of the DAS is being carried out by the Universidad Politecnica de Cartagena (UPCT) in collaboration with the IAC.

4. SCIENCE GOALS AND SCIENCE CASES

4.1 Core science

The TMS experiment has the three following primary scientific goals:

- To measure the absolute sky spectrum in the 10–20 GHz range, searching for possible deviations from a pure blackbody at the level of 10 Jy/sr. The choice of this sensitivity is driven by the expected level of distortion signal due to reionization and structure formation in our Universe.
- To provide accurate information of the spectral properties of the synchrotron and anomalous microwave emission from our Galaxy, and to constrain the emission properties of the extragalactic emission, both in the range 10–20 GHz. In particular, we aim to provide the most precise measurement of the frequency dependence of the synchrotron monopole in this frequency range, allowing us to confirm or discard the excess of emission detected by ARCADE 2.
- To provide an absolute calibration scale for the QUIJOTE experiment, as well as an accurate (sub-percent) relative calibration scale for the four QUIJOTE MFI frequencies (11, 13, 17 and 19 GHz).

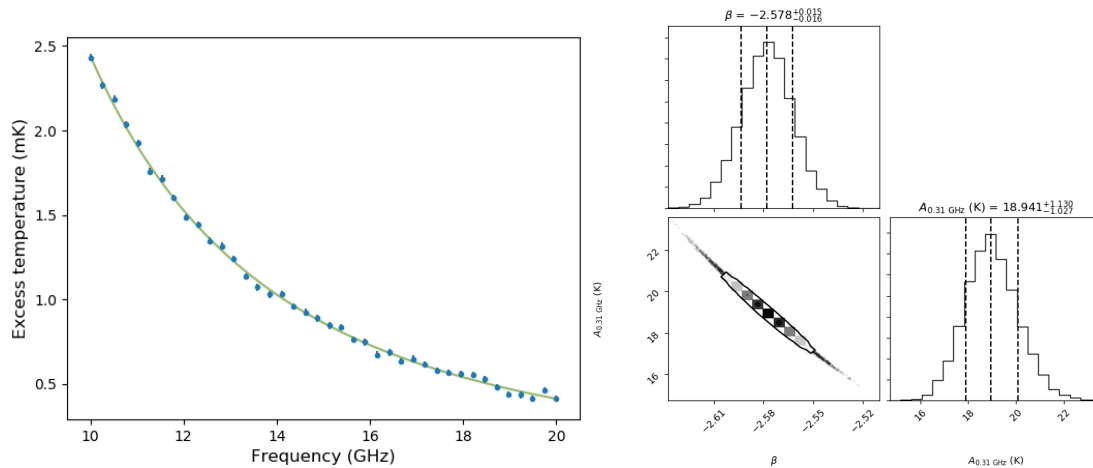


Figure 7. Left: Forecasted measurements of the ARCADE excess emission after one month of effective integration time. Right: Corner plot showing the posterior distribution functions for the two parameters β and $A_{0.31}$ parameterising the emission as $T(\nu) = A_{0.31}(\nu_{\text{GHz}}/0.31)^\beta$. The reference input data ($A_{0.31} = 18.4 \text{ K}$ and $\beta = -2.57$ from [15]), and the 1-sigma confidence intervals are shown as vertical dashed lines.

To achieve these scientific objectives, TMS will conduct two types of surveys with a sky coverage similar to that of the QUIJOTE experiment (see Figure 6).

- i) Deep survey. Dedicated raster scan observations will allow us to explore the sky area observed by ARCADE 2 (approximately $3,000 \text{ deg}^2$). After 1-month integration, we will reach sensitivities per beam of the order of $20 \mu\text{K}$, allowing us to measure the spectral dependence β of the emission with a precision of $\Delta\beta = 0.015$ (see Figure 7). After one effective year of integration in this area (or a similar patch), we will reach the level of $6 \mu\text{K}$ per beam (equivalent to 20 Jy/sr in the lowest part of the band).
- ii) Wide survey. Observations at a constant elevation of 60° will provide a continuous coverage of the sky area between declination $\delta = -1.7^\circ$ and $\delta = 58.3^\circ$, with a sky fraction of $f_{\text{sky}} = 0.44$ (equivalent to $\sim 18,200 \text{ deg}^2$). After two years of effective integration, this survey will provide sensitivities per beam of the order of $10 \mu\text{K}$ (approximately $\sim 33 \text{ Jy/sr}$ in the lowest part of the band).

Apart from the “guaranteed” science cases mentioned above, the high sensitivity of the TMS will open the window to discover possible non-expected signals in this frequency range.

4.2 Non-core science

Apart from the scientific goals described in the previous subsection, we have also identified a number of secondary science projects.

- i) Improved atmospheric model for the Teide Observatory, and characterization of the ozone lines. As a by-product, the TMS will produce instantaneous measurements of the atmospheric transparency over the Teide Observatory in the range 10–20 GHz (see left panel in Figure 8). In combination with the existing meteorological stations at the Observatory, these database could be used to refine the existing models.²⁸ Moreover, and thanks to its spectroscopic capability, the TMS will be able to resolve and accurately measure the ozone lines in the same frequency range (see right panel in Figure 8). This information will be also valuable to improve the atmospheric model of the Observatory.
- ii) Spectral energy distribution (SED) in intensity and polarization of specific Galactic regions. Thanks to the TMS polarimetric capabilities, we should be able to reconstruct the SED in some extended (compared to the beam size) regions of interest. We mention here two examples. First, the North Galactic Spur, a huge radio feature extending up to high Galactic latitudes, with a still uncertain physical origin.²⁹ And

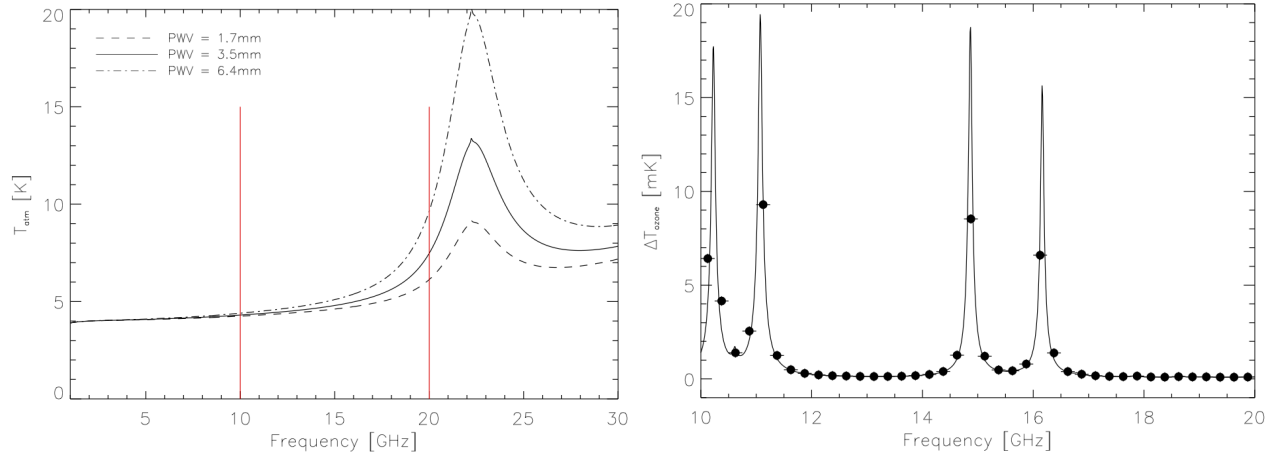


Figure 8. Left: Simulated curves of the zenith temperature T_{atm} at the Teide Observatory, for three different values of water vapour content. The models were generated using the AM code,³³ using the average pressure and temperature profiles for the Teide Observatory.²⁸ PWV values of 1.7, 3.5 and 6.4 mm correspond to the 25% percentile, median and 75% percentile of the distribution,²¹ respectively. Vertical red lines indicate the frequency range covered by TMS (10–20 GHz). Right: Predicted ozone lines in the 10–20 GHz range, as measured by the TMS after 1 min integration. The frequencies of the four main ozone features in this range are 10.23 GHz, 11.07 GHz, 14.87 GHz and 16.16 GHz.

second, the so-called WMAP Haze, an excess of microwave emission towards the Galactic centre that was found in WMAP data at 23 GHz, and which has a good spatial correlation in Gamma-rays in Fermi data.³⁰ An interesting possibility for its origin is hard synchrotron radiation driven by relativistic electrons and positrons produced by dark matter annihilation in the Galactic center.³¹ The combination of QUIJOTE data with TMS will shed light on the physical origin of these two regions.

- iii) CO line at high redshifts. The carbon monoxide molecule (CO) is present in the universe in regions of star formation, and for this reason is used as a probe for star forming activity in the radio regime thanks to its rotational transitions. These transitions must obey the selection rule $\Delta J = \pm 1$, where J is the rotational quantum number, and out of those the strongest one is the one involving the fundamental state $J = 1 \rightarrow J = 0$ at $\nu \simeq 115$ GHz. The pioneering work of Righi et al.³² provided the first estimates of the average intensity and angular fluctuations associated to these rotational transitions of the CO molecule across cosmological history. In that work, the CO radio emission was predicted to create an average intensity just below the average brightness of the CMB. But more interestingly, it was also shown that, while the angular anisotropies of the CMB and other background components like dust, free-free or synchrotron, were predicted not to be dependent upon the observing spectral resolution $\Delta\nu/\nu_{\text{obs}}$, the corresponding anisotropies associated to CO transitions (and to other any spectral line) should have a strong $\Delta\nu/\nu_{\text{obs}}$ dependence. The combination of broad band data from other experiments (like, e.g., QUIJOTE, with $\Delta\nu/\nu_{\text{obs}} \sim 0.3$) and the spectral / narrow-band observations from TMS ($\Delta\nu/\nu_{\text{obs}} \sim 0.01\text{--}0.02$) thus opens the way to constrain the presence of CO during the end of the epoch of reionization ($z \lesssim 9$).

5. PROJECT STATUS AND BASELINE

The TMS enclosure and dome are already at the Teide Observatory. The TMS platform is being fabricated by IDOM, and should arrive in spring 2021. The TMS cryostat is fabricated since mid 2019, and it is being tested at the IAC. The optomechanical components (horns, OMTs, hybrids) are now in the final design and fabrication phase. The reference load should be produced by mid 2021, and the data acquisition system based on FPGAs is now in the final development phase. We expect the commissioning of the TMS by mid 2022.

ACKNOWLEDGMENTS

The TMS experiment is being developed by the Instituto de Astrofísica de Canarias (IAC), with an instrumental participation from the INAF group (Bologna, Italy), the University of Milano (Italy), and the Universidad Politécnica de Cartagena (UPCT). Partial financial support is provided by the Spanish Ministry of Science and Innovation (MICINN), under the projects AYA2017-84185-P, IACA15-BE-3707, EQC2018-004918-P and the FEDER Agreement INSIDE-OOCC (ICTS-2019-03-IAC-12). We also acknowledge financial support of the Severo Ochoa Program SEV-2015-0548. We acknowledge the use of the Legacy Archive for Microwave Background Data Analysis (LAMBDA), part of the High Energy Astrophysics Science Archive Center (HEASARC). HEASARC/LAMBDA is a service of the Astrophysics Science Division at the NASA Goddard Space Flight Center.

REFERENCES

- [1] Rubiño-Martín, J. A., Rebolo, R., Aguiar, M., Génova-Santos, R., Gómez-Reñasco, F., Herreros, J. M., Hoyland, R. J., et al., “The QUIJOTE-CMB experiment: studying the polarisation of the galactic and cosmological microwave emissions,” in [*Ground-based and Airborne Telescopes IV*], *Society of Photo-Optical Instrumentation Engineers (SPIE) Conference Series* **8444**, 84442Y (Sept. 2012).
- [2] Hinshaw, G., Larson, D., Komatsu, E., Spergel, D. N., Bennett, C. L., Dunkley, J., Nolte, M. R., Halpern, M., Hill, R. S., Odegard, N., Page, L., Smith, K. M., Weiland, J. L., Gold, B., Jarosik, N., Kogut, A., Limon, M., Meyer, S. S., Tucker, G. S., Wollack, E., and Wright, E. L., “Nine-year Wilkinson Microwave Anisotropy Probe (WMAP) Observations: Cosmological Parameter Results,” *ApJS* **208**, 19 (Oct. 2013).
- [3] Planck Collaboration, Aghanim, N., Akrami, Y., Ashdown, M., Aumont, J., et al., “Planck 2018 results. VI. Cosmological parameters,” *A&A* **641**, A6 (Sept. 2020).
- [4] Chluba, J., Abitbol, M. H., Aghanim, N., Ali-Haïmoud, Y., Alvarez, M., Basu, K., Bolliet, B., Burigana, C., de Bernardis, P., Delabrouille, J., Dimastrogiovanni, E., Finelli, F., Fixsen, D., Hart, L., Hernandez-Monteagudo, C., Hill, J. C., Kogut, A., Kohri, K., Lesgourgues, J., Maffei, B., Mather, J., Mukherjee, S., Patil, S. P., Ravenni, A., Remazeilles, M., Rotti, A., Rubino-Martin, J. A., Silk, J., Sunyaev, R. A., and Switzer, E. R., “New Horizons in Cosmology with Spectral Distortions of the Cosmic Microwave Background,” *arXiv e-prints*, arXiv:1909.01593 (Sept. 2019).
- [5] Hill, J. C., Battaglia, N., Chluba, J., Ferraro, S., Schaun, E., and Spergel, D. N., “Taking the Universe’s Temperature with Spectral Distortions of the Cosmic Microwave Background,” *Phys. Rev. Lett.* **115**, 261301 (Dec. 2015).
- [6] André, P., Baccigalupi, C., Banday, A., et al., “PRISM (Polarized Radiation Imaging and Spectroscopy Mission): an extended white paper,” *JCAP* **2014**, 006 (Feb. 2014).
- [7] Fixsen, D. J. and Mather, J. C., “The Spectral Results of the Far-Infrared Absolute Spectrophotometer Instrument on COBE,” *ApJ* **581**, 817–822 (Dec. 2002).
- [8] Sunyaev, R. A. and Khatri, R., “Unavoidable CMB Spectral Features and Blackbody Photosphere of Our Universe,” *International Journal of Modern Physics D* **22**, 1330014 (June 2013).
- [9] Chluba, J., “Which spectral distortions does Λ CDM actually predict?,” *MNRAS* **460**, 227–239 (July 2016).
- [10] Silk, J. and Chluba, J., “Next Steps for Cosmology,” *Science* **344**, 586–588 (May 2014).
- [11] Bersanelli, M., Bensadoun, M., de Amici, G., Levin, S., Limon, M., Smoot, G. F., and Vinje, W., “Absolute Measurement of the Cosmic Microwave Background at 2 GHz,” *ApJ* **424**, 517 (Apr. 1994).
- [12] Staggs, S. T., Jarosik, N. C., Meyer, S. S., and Wilkinson, D. T., “An Absolute Measurement of the Cosmic Microwave Background Radiation Temperature at 10.7 GHz,” *ApJL* **473**, L1 (Dec. 1996).
- [13] Gervasi, M., Zannoni, M., Tartari, A., Boella, G., and Sironi, G., “TRIS. II. Search for CMB Spectral Distortions at 0.60, 0.82, and 2.5 GHz,” *ApJ* **688**, 24–31 (Nov. 2008).
- [14] Kogut, A., Fixsen, D. J., Levin, S. M., Limon, M., Lubin, P. M., Mirel, P., Seiffert, M., Singal, J., Villela, T., Wollack, E., and Wuensche, C. A., “ARCADE 2 Observations of Galactic Radio Emission,” *ApJ* **734**, 4 (June 2011).
- [15] Seiffert, M., Fixsen, D. J., Kogut, A., Levin, S. M., Limon, M., Lubin, P. M., Mirel, P., Singal, J., Villela, T., Wollack, E., and Wuensche, C. A., “Interpretation of the ARCADE 2 Absolute Sky Brightness Measurement,” *ApJ* **734**, 6 (June 2011).

- [16] Fixsen, D. J., Kogut, A., Levin, S., Limon, M., Lubin, P., Mirel, P., Seiffert, M., Singal, J., Wollack, E., Villela, T., and Wuensche, C. A., “ARCADE 2 Measurement of the Absolute Sky Brightness at 3-90 GHz,” *ApJ* **734**, 5 (June 2011).
- [17] Seiffert, M., Fixsen, D. J., Kogut, A., Levin, S. M., Limon, M., Lubin, P. M., Mirel, P., Singal, J., Villela, T., Wollack, E., and Wuensche, C. A., “Interpretation of the ARCADE 2 Absolute Sky Brightness Measurement,” *ApJ* **734**, 6 (June 2011).
- [18] Feng, C. and Holder, G., “Enhanced Global Signal of Neutral Hydrogen Due to Excess Radiation at Cosmic Dawn,” *ApJL* **858**, L17 (May 2018).
- [19] Hardcastle, M. J., Shimwell, T. W., Tasse, C., Best, P. N., Drabent, A., Jarvis, M. J., Prandoni, I., Rottgering, H. J. A., Sabater, J., and Schwarz, D. J., “The contribution of discrete sources to the sky temperature at 144 MHz,” *arXiv e-prints*, arXiv:2011.08294 (Nov. 2020).
- [20] Kogut, A., Fixsen, D. J., Chuss, D. T., Dotson, J., Dwek, E., Halpern, M., Hinshaw, G. F., Meyer, S. M., Moseley, S. H., Seiffert, M. D., Spergel, D. N., and Wollack, E. J., “The Primordial Inflation Explorer (PIXIE): a nulling polarimeter for cosmic microwave background observations,” *JCAP* **2011**, 025 (July 2011).
- [21] Castro-Almazán, J. A., Muñoz-Tuñón, C., García-Lorenzo, B., Pérez-Jordán, G., Varela, A. M., and Romero, I., “Precipitable Water Vapour at the Canarian Observatories (Teide and Roque de los Muchachos) from routine GPS,” *Observatory Operations: Strategies, Processes, and Systems VI* **9910**(May), 99100P (2016).
- [22] Watson, R. A., Carreira, P., Cleary, K., Davies, R. D., Davis, R. J., Dickinson, C., Grainge, K., Gutiérrez, C. M., Hobson, M. P., Jones, M. E., Kneissl, R., Lasenby, A., Maisinger, K., Pooley, G. G., Rebolo, R., Rubiño-Martín, J. A., Rusholme, B., Saunders, R. D. E., Savage, R., Scott, P. F., Slosar, A., Sosa Molina, P. J., Taylor, A. C., Titterton, D., Waldram, E., and Wilkinson, A., “First results from the Very Small Array - I. Observational methods,” *MNRAS* **341**, 1057–1065 (June 2003).
- [23] Bersanelli, M. et al., “Planck Pre-Launch Status: Design and Description of the Low Frequency Instrument,” *Astronomy and Astrophysics* **520**(A4) (2010).
- [24] Alonso-Arias, P., Rubiño-Martín, J. A., Hoyland, R. J., et al., “New technologies for the TMS and current status,” in [*Ground-based and Airborne Telescopes IV*], *Society of Photo-Optical Instrumentation Engineers (SPIE) Conference Series* **in press** (2020).
- [25] De Miguel Hernández, J. and Hoyland, R., “Fundamentals of horn antennas with low cross-polarization levels for radioastronomy and satellite communications,” *Journal of Instrumentation* **14**, R08001–R08001 (08 2019).
- [26] De Miguel Hernández, J., Hoyland, R., Sosa-Cabrera, D., Deviaene, S., Fuerte-Rodríguez, P., González-Carretero, E., and Vega, A., “Manufacturing of 3d-metallic electromagnetic metamaterials for feedhorns used in radioastronomy and satellite communications,” *Mechanics of Materials* **139**, 103195 (10 2019).
- [27] Rubiño-Martín, J. A. et al., “QUIJOTE scientific results - IV. A northern sky survey at 10–20 GHz with the Multi-Frequency Instrument,” *MNRAS*, *in prep.* (2020).
- [28] Otarola, A., Génova-Santos, R. T., Castro-Almazán, J. A., and Muñoz-Tuñón, C., “Model to estimate Precipitable Water Vapor (PWV) from Clear Sky QUIJOTE spectral bands optical depth,” *CUpS* **1**, 1–5 (2018).
- [29] Wolleben, M., Landecker, T. L., Reich, W., and Wielebinski, R., “An absolutely calibrated survey of polarized emission from the northern sky at 1.4 GHz. Observations and data reduction,” *A&A* **448**, 411–424 (Mar. 2006).
- [30] Dobler, G., “A Last Look at the Microwave Haze/Bubbles with WMAP,” *ApJ* **750**, 17 (May 2012).
- [31] Hooper, D., Finkbeiner, D. P., and Dobler, G., “Possible evidence for dark matter annihilations from the excess microwave emission around the center of the Galaxy seen by the Wilkinson Microwave Anisotropy Probe,” *Phys. Rev. D* **76**, 083012 (Oct. 2007).
- [32] Righi, M., Hernández-Monteagudo, C., and Sunyaev, R. A., “Carbon monoxide line emission as a CMB foreground: tomography of the star-forming universe with different spectral resolutions,” *A&A* **489**, 489–504 (Oct. 2008).
- [33] Paine, S., “The am atmospheric model,” DOI: 10.5281/zenodo.640645 (Sep 2019).